Cellular Oncology 31 (2009) 345–356
DOI 10.3233/CLO-2009-0480
IOS Press

Pla2g2a attenuates colon tumorigenesis in azoxymethane-treated C57BL/6 mice; expression studies reveal Pla2g2a target genes and pathways

Remond J.A. Fijneman [a,e,*], Lindsey K. Bade [b,h,*], Johannes R. Peham [a], Mark A. van de Wiel [c,d], Victor W.M. van Hinsbergh [e,f], Gerrit A. Meijer [a], Michael G. O'Sullivan [g] and Robert T. Cormier [b,**]

[a] *Department of Pathology, VU University Medical Center, Amsterdam, The Netherlands*
[b] *Department of Biochemistry & Molecular Biology, University of Minnesota Medical School, Duluth, MN, USA*
[c] *Department of Epidemiology and Biostatistics, VU University Medical Center, Amsterdam, The Netherlands*
[d] *Department of Mathematics, VU University, Amsterdam, The Netherlands*
[e] *Department of Medical Oncology, VU University Medical Center, Amsterdam, The Netherlands*
[f] *Department of Physiology, VU University Medical Center, Amsterdam, The Netherlands*
[g] *University of Minnesota College of Veterinary Medicine, St. Paul, MN, USA*
[h] *Genetics and Cell Biology, University of Minnesota Medical School, Minneapolis, MN, USA*

Abstract. *Background*: The group IIA secretory phospholipase A_2 gene, *Pla2g2a*, confers resistance to intestinal tumorigenesis in the $Apc^{Min/+}$ mouse model. However, it is unclear how Pla2g2a exerts its tumor-suppressive effects and whether its mode of action depends on *Apc*-germline mutations.

Methods: We tested whether expression of a *Pla2g2a* transgene provides protection against carcinogen-induced colon tumors, and examined whether the normal colon microenvironment is modulated by Pla2g2a expression.

Results: Pla2g2a strongly inhibited colon tumorigenesis in mice following treatment with the DNA alkylating agent azoxymethane (AOM). Moreover, AOM-induced duodenal tumors were also attenuated by Pla2g2a expression. These tumors demonstrated upregulation of β-catenin, indicative of involvement of the Wnt signaling pathway. Comparison of genome-wide microarray expression profiles of healthy (non-pathologic) colon tissues from Pla2g2a-transgenic to non-transgenic mice revealed 382 genes that were differentially expressed, comprising clusters of genes involved in inflammation and microbial defense, cell signaling and cell cycle, transactivation, apoptosis and mitochondrial function, DNA repair, and lipid and energy metabolism. Pathway analysis using Gene Set Enrichment Analysis (GSEA) indicated that Pla2g2a suppresses the expression of interferon-induced genes.

Conclusion: Our results demonstrate that Pla2g2a attenuates colon tumorigenesis independent of *Apc*-germline mutations, and reveal Pla2g2a target genes and pathways in non-pathologic colon microenvironment that influence conditions for colorectal cancer development.

Keywords: Colorectal cancer, Pla2g2a, microarray expression analysis, transgenic mice

1. Introduction

Treatment of rodents with the DNA alkylating carcinogen, azoxymethane (AOM), induces colon tumors that exhibit a range of molecular alterations that is similar to that observed in human colorectal cancer [4,19, 22,32,33,36,56,64,67]. Interestingly, inbred strains of mice used in AOM studies demonstrate marked differ-

[*] These authors contributed equally to the study.

[**] Corresponding author: Robert T. Cormier, Department of Biochemistry & Molecular Biology, University of Minnesota Medical School, 1035 University Drive, Duluth, MN 55812, USA. Tel.: +1 218 726 8625; Fax: +1 218 726 8014; E-mail: rcormier@d.umn.edu.

ences in susceptibility to AOM-induced tumorigenesis [11,58,66]. For example, A/J mice are highly sensitive to AOM-induced neoplasia while AKR/J mice are highly resistant. In the $Apc^{Min/+}$ mouse, a genetic model for colorectal cancer, a number of genetic modifiers have been identified. An example is the *Mom1* (Modifier of Min-1) locus [21], a complex of genes on distal chromosome four that includes the *Pla2g2a* gene, which encodes for a secretory phospholipase that is naturally mutant in the C57BL/6 mouse strain [48]. Strains of mice that carry the mutant *Pla2g2a* allele develop a severe $Apc^{Min/+}$ phenotype while strains that carry the wildtype *Pla2g2a* allele demonstrate resistance to intestinal tumorigenesis [30]. Genetic evidence for Pla2g2a's function as a suppressor of tumorigenesis was demonstrated by the reduction in tumors observed in C57BL/6 $Apc^{Min/+}$ mice carrying a wildtype *Pla2g2a* transgene derived from the AKR strain [17]. The Pla2g2a tumor resistance phenotype is strongest in the large intestine [16].

Transcription of the wild-type *Pla2g2a* transgene is driven by its endogenous promoter sequences, and spatial distribution of its expression is similar to expression of the endogenous *Pla2g2a* gene, i.e. by Paneth cells in the small intestine and by goblet cells in the large intestine [16,17,50]. The mechanisms underlying Pla2g2a's suppression of tumor development in the $Apc^{Min/+}$ mouse are not clear. Two explanations that have been proposed are: (1) Pla2g2a's bactericidal functions as a secreted molecule that may help manage the flora in the intestinal crypt lumen, thereby limiting inflammation and maintaining gut homeostasis, and (2) via the production of fatty acids and its derivatives like prostaglandins with potent signaling activity. While Pla2g2a's antimicrobial activity may indeed be shown to play a significant role in its tumor resistance, recent work has also shown that Pla2g2a is involved in complex signaling pathways that includes the Wnt/β-catenin cascade [3,23,26,62].

In the current study we extended previous work by testing whether expression of a wildtype AKR-derived *Pla2g2a* transgene in C57BL/6J mice could prevent tumor development in the AOM model of intestinal tumorigenesis. Moreover, the effects of Pla2g2a expression on normal colon were investigated by comparing genome-wide gene expression profiles of distal colon tissues obtained from C57BL/6J mice that expressed either mutant or wildtype copies of the *Pla2g2a* gene. Overall, we found that expression of Pla2g2a provided strong resistance to AOM-induced colon tumorigenesis, in both genders and at 8 and 12 months of age. In addition, we observed AOM-induction of tumors in the small intestine, principally in the duodenum, a phenotype that was also attenuated by the expression of Pla2g2a. Expression analysis identified Pla2g2a target genes that modulate cell signaling, transactivation, apoptosis, intracellular trafficking, inflammation, and intestinal metabolism were identified that suggest mechanisms underlying Pla2g2a's tumor resistance. Pathway analysis by Gene Set Enrichment Analysis (GSEA) revealed suppression of interferon-induced genes as a potentially key effect of Pla2g2a, indicating that modulation of gut immune homeostasis may underlie Pla2g2a's action.

2. Materials and methods

2.1. Mice

C57BL/6J mice were obtained from the Jackson Laboratory (Bar Harbor, ME). C57BL/6J-*Pla2g2a-Tg* mice [16] were obtained from a colony maintained at the University of Minnesota Medical School. C57BL/6J mice were crossed to C57BL/6J-*Pla2g2a-Tg* mice and all AOM test mice were littermates generated from this cross. Mice used for gene expression analysis also came from the same colony. All mice were housed and bred at the University of Minnesota Medical School Duluth Animal Services Facility (AALAC accredited) and all mouse experiments followed a protocol approved by the University of Minnesota Institutional Animal Care and Use Committee. Mice were housed in micro-isolator cages that were changed in a laminar flow hood following a customary protocol to prevent pathogen transfer. Sentinel mice caged on the same racks as experimental mice tested negative for a panel of common pathogens during the entire period of the study. All mice were fed food (Purina 5001 Rodent Chow) and tap water *ad libitum*. All mice were monitored daily for signs of distress and sacrificed when either distressed or moribund. Test mice were sacrificed at 240 and 360 days.

2.2. Azoxymethane treatment

AOM was obtained from Sigma-Aldrich (St. Louis, MO) in 100 mg vials, diluted in saline (0.9% NaCl) at a concentration of 1.25 mg/ml, and aliquots were stored frozen until use. Mice, starting at 45 days of age, were administered 10 mg AOM/kg body weight by intraperitoneal injection once per week for 6 consecutive weeks. All mice were treated with AOM blind to genotype.

2.3. Genotyping

DNA was isolated from tail snips using a Qiagen DNA Easy kit. The genotype of the *Pla2g2a* locus was determined by PCR assay as previously described [16]. PCR was performed on an Applied Biosystems GeneAmp 9700 Thermal Cycler.

2.4. Tumor analysis

All mice were sacrificed by CO_2 asphyxiation. The entire intestinal tract was removed, washed in 1X PBS and cut into five sections consisting of the large intestine (including colon and cecum) and four equal length sections of the small intestine. Each section was cut longitudinally and fixed flat overnight in 10% buffered neutral formalin between bibulous paper and 3-ply paper towel. Tissues were then transferred to 70% ethanol, further cleaned and stored in paraffin-sealed vials prior to scoring. Tumors were independently scored by two observers (L.K.B., R.T.C.) blind to the genotype of the sample using a Nikon SMZ1000 dissecting microscope at 10× magnification.

2.5. Histopathology

Histopathological analysis of tumors and adjoining normal tissue was performed on formalin-fixed tissues obtained from male and female mice from both the 240 and 360 day classes of C57BL/6J mice that were either positive or negative for the *Pla2g2a* transgene. Multiple H&E sections were obtained from tumors from the colon and duodenum. All tissues were analyzed blind to the genotype of the samples by an A.C.V.P.-certified veterinary pathologist (M.G.O'S.) from the University of Minnesota Cancer Core Histopathology Shared Resources facility and using the standardized nomenclature of the 2003 Consensus Report and Recommendations for pathology of mouse models of intestinal cancer as published [12].

2.6. Immunohistochemistry

4 μm formalin-fixed, paraffin-embedded sections of small intestinal tumors were deparaffinized and rehydrated, followed by antigen retrieval using 10 mM Citrate buffer pH 6.0 in the Biocare Decloaking Chamber (electric pressure cooker) (Biocare, Walnut Creek, CA). Immunohistochemistry for β-catenin was performed on a Dako Autostainer (Dako, Carpinteria, CA) using a goat anti-human β-catenin polyclonal antibody (Santa Cruz Biotechnology, Santa Cruz, CA) as primary antibody (after blocking endogenous peroxidase and application of a protein block), with detection by a biotinylated donkey anti-goat antibody (Jackson ImmunoResearch Laboratories, West Grove, PA) and streptavidin-linked horse radish peroxidase (Dako) using diaminobenzidine (Dako) as the chromogen. Mayer's Hematoxylin (Dako) was used as the counterstain. Small intestinal adenomas from $Apc^{Min/+}$ mice were used as a positive control tissue, and for negative control slides the primary antibody was substituted with Super Sensitive Goat Negative Serum (Biogenex, San Ramon, CA).

2.7. Tumor statistical analysis

Two-sided P values for tumor counts were determined by use of Student's t-test comparing gender and age-matched classes produced in the same genetic crosses.

2.8. RNA extraction and quality control

The colon of mice was removed, cut longitudinally, cleaned in PBS and stored in Qiagen RNA Later (Valencia, CA). Using a polytron homogenizer, about 1 cm of tissue was homogenized in TRIzol reagent (Invitrogen, Paisley, UK). Total RNA was isolated following the manufacturer's protocol. RNA concentrations were measured with a Nanodrop spectrophotometer (ND-1000, NanoDrop Technologies; Wilmington, DE) and treated with RNase-Free DNase (Promega, Madison, WI). The quality of RNA preparations was assessed with a lab-on-a-chip 2100 Bioanalyzer (Agilent Technologies, Wilmington, DE). All samples used for microarray analysis had an RNA integrity number (RIN value) of 7 or higher, following the manufacturer's recommendations.

2.9. Oligonucleotide microarray and data analysis

Two-color microarray-based gene expression analysis was carried out using Agilent 4 × 44K whole mouse genome microarrays (G4122F, Agilent Technologies, Wilmington, DE). This array includes more than 41,000 mouse genes and transcripts. Per sample, 500 ng of RNA was spiked, labeled, amplified, and hybridized using Agilent reagents, according to Agilent Gene Expression oligo microarrays protocol (version 5.0.1). For each group (transgenic and non-transgenic) half of the samples were labeled with Cy3

and half of the samples with Cy5, to prevent bias of the data due to labeling with these fluorescent dyes. Arrays were scanned using an Agilent Microarray Scanner, and the intensity of fluorescent images was quantified using Agilent Feature Extraction software (version 9.1.3). Pre-processing of data, quality checks, and significance analysis were all performed using the R-Bioconductor [28] package using 'limma' [63]. Differential expression of genes was quantified by the moderated t-statistic. Raw P-values were adjusted for multiple testing by using the Benjamini–Hochberg [9] false discovery rate (FDR) correction. Genes with adjusted P-value smaller or equal to 0.1 were declared to be significant. A detailed description of the microarray data analysis is provided in the *Supplementary Methods*. The analysis R-scripts are available upon request from the authors (M.A. van de Wiel). Following this protocol, RNA expression profiles from the colon of 6 C57BL/6J-*Pla2g2a-Tg* mice (3 females, 3 males) and 4 C57Bl/6J mice (2 females, 2 males) were analyzed, and differentially expressed genes, allowing for gender, were identified. Functional classification of these genes and pathway analysis were carried out using Ingenuity Pathways Analysis software (www.ingenuity.com), provided through the University of Minnesota Supercomputing Institute. In addition, GSEA was used as a computational method to identify sets of genes with coordinate differences in gene expression (GSEA v2.0, http://www.broad.mit.edu/gsea/) [54,65]. Gene sets analyzed were obtained from the Molecular Signatures Database (MSigDB_v2.5, http://www.broad.mit.edu/gsea/msigdb/index.jsp) and comprised curated gene sets, motif gene sets, and Gene Ontology (GO) gene sets, i.e. collections c2, c3 and c5. Default settings were used, except for 'Collapse dataset to gene symbols' (set to 'false'), 'Permutation type' (set to 'gene_set'), and the 'Max size' of gene sets (set to '1500'). Gene sets with a family-wise error rate FWER < 0.05, which is used as a conservative correction factor that aims to exclude even a single false-positive gene set [65], were considered significant.

2.10. Quantitative real time PCR

RNA was made as described above or with RNAeasy Plus Mini Kit with gDNA Eliminator (Qiagen). cDNA was synthesized using the GeneAmp Gold RNA PCR Core Kit (Applied Biosystems). SYBR green real time PCR assays employed the Power SYBR Green PCR Master Mix (Applied Biosystems). The expression level of each gene was determined in triplicate by real time PCR in the 7900HT Sequence Detection System (Applied Biosystems). After PCR amplification in the thermocycler, a C_t value was determined for each sample. The relative amount of mRNA for each gene was determined by comparing the C_t value of the control and treated samples after normalization with the GAPDH internal control gene. All real time PCR work was performed by ACGT Inc. (Wheeling, IL, USA) except for Pla2g2a, whose overexpression in C57BL/6J-*Pla2g2a-Tg* mice compared to C57BL/6J mice was previously determined by ACTG Inc. on a Muc2-deficient background [25], and now determined by our lab using the qRT–PCR protocol described by Carvalho et al. [14]. Primer sequences are as follows: Nudt-F GTGCACAGCGA GACCAAGTA; Nudt-R TTTGCAAAGTTGCTGGT GAG; Aldh2-F TGTCAGGGAGTGGCAGGG; Aldh2-R CGGGCTG AGGAAGCAGG; Klk7-F TGTGCTCGGATGTGAA GCTCATCT; Klk7-R GTCACCATTGCACGTGTTG GTCTT; Mier2-F GTCAGACCCCATCTCTGAGC; Mier2-R TCTTCTTCCCCAGAAAGCAA; Rab5c-F ACGGGCTAAGAATTGGGTGAAGGA; Rab5c-R TCTGCATAGGCTTGTGCTTCCTGA; Map3k10-F AGTTCCACTTTGCAGAAGGAGCGA; Map3k10-R CATCTGCCTCCGCAAATTCTTCCA; Adam11-F GTGCACAGCGAGACCAAGTA; Adam11-R TTTG CAAAGTTGCTGGTGAG; Yap1-F GCGCCTATGAT TGGCCAG; Yap1-R GATAAGGTCAGAGAGCACT GTCAGG; Ercc2-F AAGCCCCTCAGGTTCTGTGC TGAA; Ercc2-R CTTGGCGTAAGTGCTGACGAG AGT; Ccr3-F CGTTCCCAGGTGGTGGAC; Ccr3-R CCTCCTACAACACTTGTGACATCC; Nfkbil1-F AC GGAAGGAAGCAAGGTCG; Nfkbil1-R GGTTAGA GCCTCCCCCACC; EphB2-F AGCAACCTGGTGT GTAAGGTGTCT; EphB2-R ATGACGATGCCATAG CTCCACACA; Dock8-F ACTGTGCAGCCGATGAG GAAGTTA; Dock8-R TTGAACCTGGCGCATCAC TATTGC; Pla2g2a-F CACCACTCCACTGCCTTGA AT; Pla2g2a-R GCAGGAAGTTGGATGCCAA; Sema7a-F TTCTAAGTACCATTACCAGAAAGTGG TC; Sema7a-R CCCTGATTCCACCACCTTGT.

3. Results

3.1. Effect of Pla2g2a on AOM-induced colon tumors

Similar to the phenotype observed in the $Apc^{Min/+}$ mouse model [16,17], expression of Pla2g2a provided strong resistance to colon tumorigenesis in

Table 1
Tumor multiplicity and incidence

Class	Age (d)	N	LI mean	Incidence (%)	SI mean	Incidence (%)
B6 males	240	10	1.6 ± 2.5	50	0.8 ± 0.9	46
B6-Pla2g2a-Tg males	240	19	0^{1}	0	0.05 ± 0.2^{3}	5
B6 females	240	11	1.4 ± 1.9	46	1.5 ± 2.4	36
B6-Pla2g2a-Tg females	240	34	0.2 ± 0.1^{2}	21	0.1 ± 0.3^{4}	9
B6 males	360	9	1.3 ± 1.3	63	0.8 ± 1.4	62
B6-Pla2g2a-Tg males	360	9	$0.4 \pm 0.7^{*}$	33	$0.2 \pm 0.4^{*}$	22
B6 females	360	12	1.8 ± 2.9	54	0.8 ± 0.7	62
B6-Pla2g2a-Tg females	360	12	$0.3 \pm 0.4^{*}$	27	$0.3 \pm 0.6^{*}$	18

Notes: p values: $^{1}p = 0.008$; $^{2}p = 0.001$; $^{3}p = 0.002$; $^{4}p = 0.002$, $^{*}p < 0.05$. Two-sided p values for tumor counts were determined by use of Student's t-test comparing gender and age-matched classes produced in the same genetic crosses. LI – large intestine, SI – small intestine.

mice treated with AOM (Table 1). At 240 days male C57BL/6J mice developed 1.6 colon tumors on average with a tumor incidence of 50%. Strikingly, *none* of the 19 male C57BL/6J-*Pla2g2a-Tg* mice treated with AOM developed a colon tumor. In female mice, there was a 7-fold reduction in colon tumors at 240 days with female C57BL/6J mice developing a mean of 1.4 tumors (46% tumor incidence), compared with 0.2 tumors (21% tumor incidence) in C57BL/6J-*Pla2g2a-Tg* mice. At 360 days, there was a similar pattern of tumor resistance, although male C57BL/6J-*Pla2g2a-Tg* mice did start to develop some colon tumors at 360 days (0.4 tumors vs. 1.3 tumors in non-transgenics). In female mice there was a similar reduction in tumors at 360 days (1.8 tumors in C57BL/6J mice vs. 0.3 tumors in C57BL/6J-*Pla2g2a-Tg* mice). We examined the size of colon tumors at 240 and 360 days but did not observe any noticeable differences in sizes (data not shown). We also investigated whether expression of Pla2g2a modulated the progression of tumors. We examined 19 colon tumors from C57BL/6J mice (11 tumors from 240 days and 8 tumors from 360 days) and 12 tumors from C57BL/6J-*Pla2g2a-Tg* mice (6 tumors at 240 days and 6 tumors from 360 days). Only 1 neoplasm (out of the total of 37) was judged to be an adenocarcinoma and this came from the C57BL/6J non-transgenic group.

3.2. Development of AOM-induced duodenal tumors

In addition to induction of colon tumorigenesis AOM also induced the formation of tumors in the small intestine, principally in the duodenum (Fig. 1, panels A and B). These tumors were predominantly small sessile or broad based adenomas, with some lesions appearing somewhat pedunculated; dysplastic epithelium was arranged predominantly in branching tubules. Some tumors also had a central flattened area giving a cup-like appearance on cross section. Histopathological analysis of 24 of these tumors (18 from C57BL/6J mice and 6 from Pla2g2a transgenics) did not find any tumors that were invasive. To investigate involvement of the Wnt-signaling pathway in AOM-induced small intestinal tumors we evaluated the expression of β-catenin by immunohistochemistry. We found increased expression of β-catenin in the tumors, as reflected in increased intensity of stain within epithelial cells of the tumors (Fig. 1, panels C and D); also notable was increased expression of β-catenin in the nuclei of tumor cells (Fig. 1, panel D).

Similar to its effect in the colon expression of Pla2g2a conferred resistance to tumorigenesis in the small intestine, although the reduction in tumor numbers was smaller at 360 days. At 240 days, male C57BL/6J mice developed 0.8 tumors on average in the small intestine with a tumor incidence of 46%, compared with 0.05 tumors (just 1 tumor in 19 mice) in the male C57BL/6J-*Pla2g2a-Tg* mice. In female mice at 240 days the averages were 1.5 tumors (36% incidence) in C57BL/6J mice compared with 0.1 tumors (9% incidence) in the C57BL/6J-*Pla2g2a-Tg* mice. However, at 360 days the C57BL/6J-*Pla2g2a-Tg* mice developed a few more tumors than at 240 days. C57BL/6J males developed 0.8 tumors (62% incidence) compared with 0.2 tumors (22% incidence) in C57BL/6J-*Pla2g2a-Tg* mice. For female mice at 360 days the mean tumor averages were 0.8 (62% incidence) for C57BL/6J mice and 0.3 (18% incidence) for the C57BL/6J-*Pla2g2a-Tg* mice. Tumor sizes in the small intestine were not significantly different between classes (data not shown).

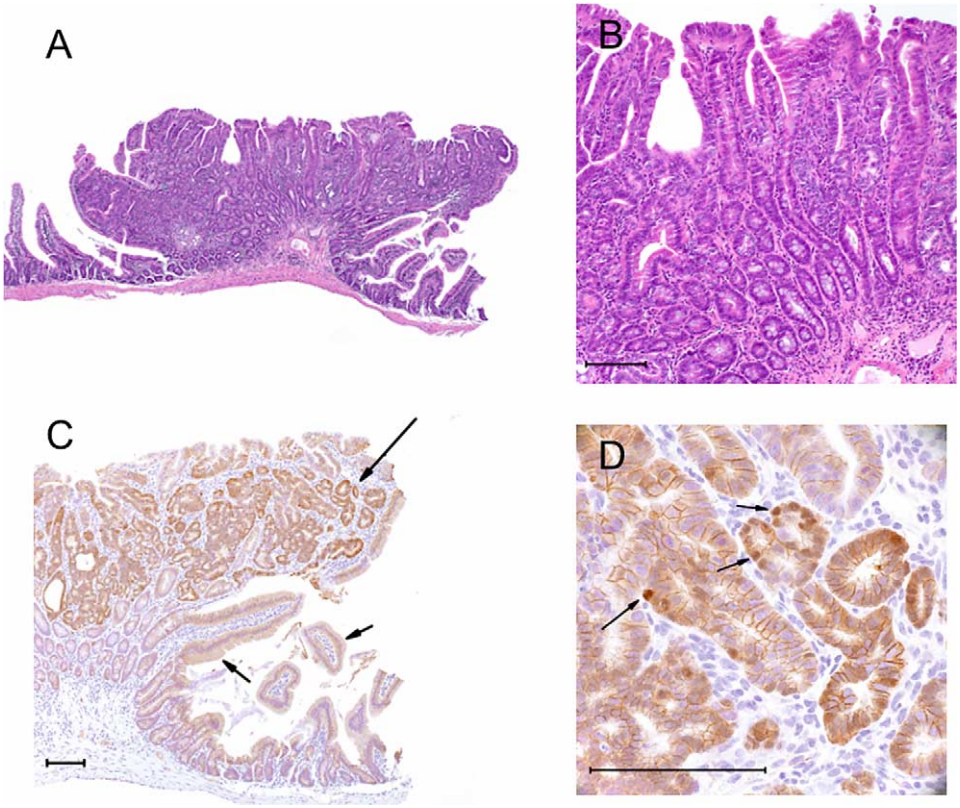

Fig. 1. (A) AOM-induced polypoid mass present in the small intestine; hematoxylin and eosin stain. (B) Higher magnification of tumor showing arrangement of cells in branching tubules; hematoxylin and eosin stain, bar = 100 μm. (C and D) Immunohistochemistry for β-catenin using DAB as chromogen and Mayer's hematoxylin as counterstain; all bars = 100 μm. (C) note light staining of normal epithelium (short arrows) compared to more intense staining of tumor (indicated by long arrow). (D) Higher magnification showing prominent nuclear staining for β-catenin (see arrows) in addition to cytoplasmic staining.

3.3. Identification of Pla2g2a target genes and pathways

To investigate the genetic pathways underlying the suppressive effects of Pla2g2a on carcinogenesis we conducted microarray expression studies using gender-matched distal normal colon tissues obtained from colony littermates that were not treated with AOM. Non-pathologic colon tissue was chosen because we hypothesized that the effects of Pla2g2a influence the colon microenvironment, thereby generating conditions that attenuate tumor development. The mice were sacrificed at 100 days of age. This age was chosen because it provided a snapshot of gene expression at the age where the tumor induction protocol is completed in AOM-treated littermates, hence a timepoint where the gene expression profiles are most likely to reveal their differential effects on tumor development. We found that Pla2g2a significantly altered expression levels of 420 transcripts, representing 382 genes ($\sim$1% of the $>$41,000 genes and transcripts on the Agilent microarray), based on use of the adjusted P value statistic. A complete list of differentially expressed genes, grouped by functional classification is found in Suppl. Table 1: http://www.qub.ac.uk/isco/JCO. Our microarray analysis revealed clusters of significantly altered genes involved in inflammation, stress response and microbial defense (*Sema7a*, *Nfkbil1*, *Ccr3*, *Syvn1*, *Adam11*, *Ifng*, *IL17ra*, *Cx3cl1*, *Map3k10*), cell signaling and cell cycle (*EphB2*, *Rgs3*, *Zfyve9*, *Taok1*, *Ncor2*), transactivation (*Runx1*, *Mier2*, *Hoxb9*, *Lhx1*, *Cdx2*, *Klf16*), apoptosis and mitochondrial function (*Yap1*, *Bax*, *Vdac1*, *Map3k10*, *Birc6*, *Ak2*, *Arl6ip5*), gastrointestinal lipid and energy metabolism (*Klk7*, *Srebf2*, *B3galt1*, *Ehbp1*, *Neto1*, *Pecr*), cellular trafficking, morphology and migration (*Rab5c*, *Dock8*) and DNA repair and protection against mutagenesis (*Ercc2*, *Nudt15*, *Aldh2*, *Parp1*, *Parp2*). Differential expression of a subset of the most significant genes from each functional group (and for which reliable primers

Table 2
qRT–PCR of genes significantly changed in microarray expression studies

Gene	Microarray (fold change)	p-value (array)	qRT–PCR (fold change)
Nudt15	3.7	5.1×10^{-8}	12.0
Aldh2	2.8	8.6×10^{-8}	1.5
Pla2g2a	26.0	9.9×10^{-8}	181.0
Klk7	2.8	3.1×10^{-7}	8.0
Mier2	3.3	3.3×10^{-7}	3.4
Rab5c	3.0	5.2×10^{-7}	1.6
Map3k10	2.3	1.0×10^{-6}	2.0
Adam11	1.9	1.5×10^{-6}	5.8
Yap1	2.5	7.0×10^{-6}	7.6
Ercc2	2.0	8.3×10^{-6}	1.8
Sema7a	1.6	2.7×10^{-5}	3.8
Dock8	2.5	3.0×10^{-5}	2.8
Nfkbil1	1.4	4.3×10^{-5}	1.5
EphB2	1.7	6.0×10^{-5}	1.5
Ccr3	1.7	7.2×10^{-5}	8.7

Note: qRT–PCR – quantitative reverse transcriptase–polymerase chain reaction.

were identified) was confirmed by quantitative reverse transcriptase–polymerase chain reaction (qRT–PCR) (Table 2).

Changes in biological processes are often accompanied by coordinate variation in expression of sets of genes. We applied GSEA to identify gene sets that were differentially expressed in normal colon from C57BL/6J-*Pla2g2a-Tg* mice compared to normal colon of C57BL/6J mice. Pre-defined gene sets were obtained from the Molecular Signatures Database (MSigDB_v2.5) and comprised curated gene sets, motif gene sets, and gene ontology (GO) gene sets. Using the family-wise error rate as a conservative correction factor (FWER < 0.05), a total of 24 gene sets were identified that exhibited significant differential expression (Table 3). Notably, the most common biological pathways identified concerned the expression of interferon (IFN)-induced genes. Gene sets #1–12 all share genes that are induced by IFNα [10,13,20,46,59, 68,73], while gene set #13 involves genes induced by IFNγ [61]. The important role of IFN-induced genes was further underscored by identification of the Interferon Regulatory Factor-2 (IRF2) motif (gene set #21), indicative of genes with an IRF2 recognition site in their promoter region within 2 kb of the gene transcription start site. Moreover, differences were observed for genes induced by TNFα (gene sets #14 and 15) [47,61], and the GO gene sets for chemokines and chemokine receptor binding (gene sets #22–24). In addition, significant differences were observed related to epithelial to mesenchyme transition (EMT; gene sets #16 and 17) [40], and to proliferation/cell cycle (gene sets #18–20) [18,29,71], the latter all sharing genes involved in spindle formation.

4. Discussion

In our current study we extended previous work using the *Apc*$^{\mathrm{Min}/+}$ mouse model by asking whether expression of Pla2g2a could prevent the development of colon tumors in the AOM model. We found that Pla2g2a provided strong tumor resistance, virtually eliminating AOM-induced tumors at 240 days. This was true in both male (0 tumors in 19 mice) and female mice (6 tumors in 34 mice), and in mice aged to both 240 and 360 days. A novel observation (in mice), was our observation of tumors in the small intestine at a frequency approaching their incidence and multiplicity in the colon. These tumors are primarily adenomas that form in the duodenum. Immunohistochemical analysis using a polyclonal antibody against β-catenin showed increased expression of β-catenin in these tumors. Previous AOM studies in mice failed to observe these tumors, possibly due to strain differences. C57BL/6 mice are relatively resistant to AOM-induced colon tumors and thus many previous studies have used tumor sensitive strains such as A/J. It is known that C57BL/6 mice are susceptible to tumors in the small intestine in *Apc*-deficient models such as the *Apc*$^{\mathrm{Min}/+}$ mouse and that the related strain B10.O20/Dem carries the susceptible allele of *ssic1* [24], a tumor susceptibility locus for ENU-induced small intestinal cancer for which *Pla2g2a* is a candidate gene. Thus C57BL/6 may carry susceptibility alleles for AOM-induced tumor formation in the small intestine. Our data support *Pla2g2a* being one potential AOM susceptibility gene for carcinogen-induced small intestinal cancer.

In parallel to the AOM study we conducted microarray expression analysis of non-pathologic colon of untreated littermates of both genotypes and both genders, to examine the effects of Pla2g2a expression on the colon microenvironment. In all we found 382 genes that are differentially expressed in *Pla2g2a* transgenic mice compared with C57BL/6J non-transgenic littermates. Pla2g2a target genes represent a broad range of molecules that are involved in induction of apoptosis, inflammation and immune response, transactivation and cell signaling, intracellular trafficking and intestinal lipid and energy metabolism. Of these groups,

Table 3
Gene sets that are more highly expressed in colon of C57BL/6J mice compared to colon of C57BL/6J-Pla2g2a-Tg mice

Set #	Collection[1]	Name of gene set[1] [Ref.]	Gene set comprises	Size	ES[2]	NES[3]	FDR q-value[4]	FWER p-value[5]
1	Curated (c2)	TAKEDA_NUP8_HOXA9_3D_UP [68]	IFNα-induced genes	105	−0.63	−2.52	<0.001	<0.001
2	Curated (c2)	TAKEDA_NUP8_HOXA9_8D_UP [68]	IFNα-induced genes	77	−0.62	−2.30	<0.001	<0.001
3	Curated (c2)	TAKEDA_NUP8_HOXA9_10D_UP [68]	IFNα-induced genes	91	−0.60	−2.33	<0.001	<0.001
4	Curated (c2)	TAKEDA_NUP8_HOXA9_16D_UP [68]	IFNα-induced genes	83	−0.57	−2.18	<0.001	0.004
5	Curated (c2)	BENNETT_SLE_UP [10]	IFNα-induced genes	16	−0.83	−2.26	<0.001	<0.001
6	Curated (c2)	DAC_BLADDER_UP [46]	IFNα-induced genes	18	−0.81	−2.22	<0.001	0.002
7	Curated (c2)	CMV_HCMV_TIMECOURSE_12HRS_UP [13]	IFNα-induced genes	16	−0.84	−2.25	<0.001	<0.001
8	Curated (c2)	IFNA_HCMV_6HRS_UP [13]	IFNα-induced genes	25	−0.77	−2.25	<0.001	<0.001
9	Curated (c2)	CMV_8HRS_UP [73]	IFNα-induced genes	22	−0.76	−2.25	<0.001	<0.001
10	Curated (c2)	IFN_ALPHA_UP [20]	IFNα-induced genes	29	−0.78	−2.41	<0.001	<0.001
11	Curated (c2)	DER_IFNA_UP [20]	IFNα-induced genes	42	−0.69	−2.29	<0.001	<0.001
12	Curated (c2)	RADAEVA_IFNA_UP [59]	IFNα-induced genes	26	−0.70	−2.06	0.002	0.034
13	Curated (c2)	SANA_IFNG_ENDOTHELIAL_UP [61]	IFNγ-induced genes	29	−0.71	−2.14	<0.001	0.010
14	Curated (c2)	SANA_TNFA_ENDOTHELIAL_UP [61]	TNFα-induced genes	44	−0.70	−2.36	<0.001	<0.001
15	Curated (c2)	LINDSTEDT_DEND_8H_VS_48H_UP [47]	TNFα-induced genes	47	−0.65	−2.23	<0.001	<0.001
16	Curated (c2)	EMT_UP [40]	TGFβ-induced EMT[6]	44	−0.62	−2.10	0.001	0.017
17	Curated (c2)	JECHLINGER_EMT_UP [40]	TGFβ-induced EMT[6]	42	−0.64	−2.14	<0.001	0.010
18	Curated (c2)	ZHAN_MM_CD138_PR_VS_REST [71]	Spindle formation	26	−0.71	−2.14	<0.001	0.010
19	Curated (c2)	GOLDRATH_CELLCYCLE [29]	Spindle formation	21	−0.73	−2.08	0.002	0.026
20	Curated (c2)	CROONQUIST_IL6_STARVE_UP [18]	Spindle formation	25	−0.71	−2.07	0.002	0.027
21	Motif (c3)	V$IRF2_01	IFN-induced genes	77	−0.52	−1.97	0.020	0.013
22	GO (c5)	CHEMOKINE_RECEPTOR_BINDING	Chemokine signaling	22	−0.74	−2.15	0.001	0.003
23	GO (c5)	G_PROTEIN_COUPLED_RECEPTOR_BINDING	Chemokine signaling	27	−0.72	−2.17	0.002	0.003
24	GO (c5)	CHEMOKINE_ACTIVITY	Chemokine signaling	21	−0.76	−2.18	0.004	0.003

[1]Obtained from the Molecular Signatures Database (MSigDB_v2.5, http://www.broad.mit.edu/gsea/msigdb/index.jsp).
[2]GSEA enrichment score.
[3]GSEA normalized enrichment score.
[4]False discovery rate.
[5]Family-wise error rate.
[6]Epithelial-to-mesenchymal transition.

genes involved in transactivation and cell signaling, especially transcription factors, represents the largest category. Among this list of genes are a number that have been previously reported or proposed to function as tumor suppressors in the colon and which are upregulated by Pla2g2a, including *EphB2* [15], *Cdx2* [37], *Bax* [69], *Klhl12* [5] and *Stk4* [53]. Similarly, Pla2g2a down regulated a group of genes that may be oncogenic, including *Nrg1* [2] and *Twist1* [70].

Pla2g2a is a Wnt/β-catenin target gene that is expressed in the secretory cell lineage, by the Paneth and goblet cells in the small intestine and by the goblet cells in the large intestine. Our microarray data suggest that Pla2g2a may function as a link between several of the canonical signaling pathways in the GI tract. For example, Pla2g2a alters the expression of a number of genes involved (directly or indirectly) in *both* the Wnt/β-catenin (*Mdfi*, *Klhl12*, *Fut8*, *Vangl2*, *Fzd8*, *EphB2*, *Fus*, *Ptk7*, *Parp1*, *Rab5c*, *Sost*) and the Notch (*Gja1*, *Mapk8ip1*, *Sh3d19*, *Cdx2*, *Ifng*, *Stat1*, *Runx1*, *Lhx1*, *Yap1*, *Smo*, *Ncor2*) signaling pathways, involved in maintenance of the stem cell compartment and in lineage specification in the mammalian gut. Pla2g2a and EphB2 have been linked in several reports over the past three years. EphB2 is a member of the Eph family of receptor tyrosine kinases and it is also a β-catenin target gene [8]. EphB2 expression is lost in some advanced human cancers but is also upregulated (like Pla2g2a) in some early stage intestinal adenomas in humans. Pla2g2a and EphB2 are co-regulated in both human colorectal and gastric cancers [3,44], Pla2g2a and EphB2 are both up regulated in mouse intestinal adenomas [57,62], and EphB2, like Pla2g2a, has also been demonstrated to be a potent tumor suppressor in mouse GI cancer models [7,15]. In gastric cancers, Aggarwal and colleagues in the group of Patrick Tan have described a set of 10 genes that reside in the "Pla2g2a neighborhood" [3], that include *EphB2* and *Ctnnb1* (β-catenin). Two other genes in the neighborhood are *Lmo4* and *Cpa2*, both differentially expressed in *Pla2g2a* transgenic colon. *Lmo4* (*Lim* homeobox gene 4), which is up regulated by Pla2g2a, has been reported to induce expression of *BMP7*, part of the TGFβ signaling pathway. More recent work by the same group of investigators has shown that in human gastric cancer PLA2G2A acts downstream of β-catenin and inhibits gastric cancer metastasis via down regulation of S100A4, a potent pro-metastatic and pro-inflammatory factor [26].

We aimed to further exploit the biological processes that are influenced by Pla2g2a in the colon by pathway analysis, using GSEA. In total, 24 gene sets were identified that exhibited significant differential expression (Table 3). Due to overlapping composition of several of these gene sets, the number of biological processes they point to is less diverse. Most of the curated gene sets revealed enrichment for differential expression of genes that can be induced by IFNα [10, 13,20,46,59,68,73]. Other curated gene sets pointed to induction of gene expression by IFNγ and/or TNFα [47,61]. These findings are further supported by identification of the IRF2 (Interferon Regulatory Factor-2) motif gene set. The GO-derived gene sets all point towards chemokine signaling, which is also indicative for leukocyte migration and immune regulation. Because all of these pathways were higher expressed by normal colon of C57BL/6J mice compared to colon of C57BL/6J-*Pla2g2a-Tg* mice, collectively they indicate that expression of Pla2g2a attenuates basal levels of immune activation. In addition, identification of two largely overlapping gene sets reflecting epithelial to mesenchyme transition (EMT), a profile that is based on exposure of epithelial cells to TGFβ [40], provided additional support for the notion that Pla2g2a may suppress metastatic behavior [26].

Quantitative RT–PCR validation analysis of a subset of the most significant genes identified in the arrays, chosen from different functional groups, confirmed the pathway analysis. Genes involved in inflammatory responses (and further linked to cytokine, chemokine, NF-κB and interferon signaling) included *Adam11* [6], *Nfkbil1* [31,60], *Sema7a* [38], *Map3k10* [41,42] and *Ccr3* [1,35]. Another group of genes confirmed by qRT–PCR were either directly involved in DNA repair such as *Ercc2* [72], or more indirectly in protection against cellular damage, such as *Aldh2* [27,51,55] and *Nudt15* [52]. Several other genes confirmed by qRT–PCR are part of canonical signaling pathways in the GI tract such as Wnt/β-catenin (*EphB2* [8], *Rab5c*); Notch (*Yap1* [43,45]), and TGFβ, Hedgehog and EMT (*Map3k10* [41,42]). Notably, several of these qRT–PCR genes have previously been linked to resistance to human colorectal cancer, including *Ercc2*, *Aldh2* and *EphB2*, and other genes on the list such as *Adam11* and *Dock8* have been reported to be down regulated in other types of cancers, such as in breast and lung.

Considered together, expression of Pla2g2a attenuates tumor development in the small and large intestine independent of *Apc*-germline mutations. This finding is further supported by the observation that Pla2g2a (directly or indirectly) influences expression of numerous genes in normal (non-pathologic) colon, including

genes involved in the Wnt/β-catenin, Notch, and possibly the TGFβ and Hedgehog pathways. These data suggest that modulation of these key-signaling pathways, involved in proliferation and differentiation of (colon crypt) stem cells, is one mechanism in which Pla2g2a attenuates tumor development. GSEA pathway analysis supports the notion that Pla2g2a contributes to maintenance of gut immune homeostasis, suggesting that prevention of chronic inflammation, mediated by inhibition of interferons, NF-κB and TNFα activity, is another mechanism in which it reduces tumor incidence [34,39,49]. However, what cells initially respond to Pla2g2a and how their effects shape the colon microenvironment remains to be elucidated.

Acknowledgements

Funding to support this study was provided by the University of Minnesota Medical School (R.T.C.) and by the 1st AEGON International Scholarship in Oncology (R.J.A.F.). We acknowledge M. Tijssen and P. Eijk for their excellent technical assistance.

References

[1] T. Adachi, C.H. Cui, A. Kanda et al., Activation of epidermal growth factor receptor via CCR3 in bronchial epithelial cells, *Biochem. Biophys. Res. Commun.* **320** (2004), 292–296.

[2] L. Adam, A. Mazumdar, T. Sharma et al., A three-dimensional and temporo-spatial model to study invasiveness of cancer cells by heregulin and prostaglandin E2, *Cancer Res.* **61** (2001), 81–87.

[3] A. Aggarwal, D.L. Guo, Y. Hoshida et al., Topological and functional discovery in a gene coexpression meta-network of gastric cancer, *Cancer Res.* **66** (2006), 232–241.

[4] W. Aizu, G.S. Belinsky, C. Flynn et al., Circumvention and reactivation of the p53 oncogene checkpoint in mouse colon tumors, *Biochem. Pharmacol.* **72** (2006), 981–991.

[5] S. Angers, C.J. Thorpe, T.L. Biechele et al., The KLHL12-Cullin-3 ubiquitin ligase negatively regulates the Wnt-beta-catenin pathway by targeting Dishevelled for degradation, *Nat. Cell Biol.* **8** (2006), 348–357.

[6] D. Atanackovic, Y. Cao, J.W. Kim et al., The local cytokine and chemokine milieu within malignant effusions, *Tumour Biol.* **29** (2008), 93–104.

[7] E. Batlle, J. Bacani, H. Begthel et al., EphB receptor activity suppresses colorectal cancer progression, *Nature* **435** (2005), 1126–1130.

[8] E. Batlle, J.T. Henderson, H. Beghtel et al., Beta-catenin and TCF mediate cell positioning in the intestinal epithelium by controlling the expression of EphB/ephrinB, *Cell* **111** (2002), 251–263.

[9] Y. Benjamini and Y. Hochberg, Controlling the false discovery rate: a practical and powerful approach to multiple testing, *J. Roy. Stat. Soc. B* **57** (1995), 289–300.

[10] L. Bennett, A.K. Palucka, E. Arce et al., Interferon and granulopoiesis signatures in systemic lupus erythematosus blood, *J. Exp. Med.* **197** (2003), 711–723.

[11] A. Bissahoyo, R.S. Pearsall, K. Hanlon et al., Azoxymethane is a genetic background-dependent colorectal tumor initiator and promoter in mice: effects of dose, route, and diet, *Toxicol. Sci.* **88** (2005), 340–345.

[12] G.P. Boivin, K. Washington, K. Yang et al., Pathology of mouse models of intestinal cancer: consensus report and recommendations, *Gastroenterology* **124** (2003), 762–777.

[13] E.P. Browne, B. Wing, D. Coleman et al., Altered cellular mRNA levels in human cytomegalovirus-infected fibroblasts: viral block to the accumulation of antiviral mRNAs, *J. Virol.* **75** (2001), 12319–12330.

[14] B. Carvalho, C. Postma, S. Mongera et al., Multiple putative oncogenes at the chromosome 20q amplicon contribute to colorectal adenoma to carcinoma progression, *Gut* **58** (2009), 79–89.

[15] H. Clevers and E. Batlle, EphB/EphrinB receptors and Wnt signaling in colorectal cancer, *Cancer Res.* **66** (2006), 2–5.

[16] R.T. Cormier, A. Bilger, A.J. Lillich et al., The Mom1AKR intestinal tumor resistance region consists of Pla2g2a and a locus distal to D4Mit64, *Oncogene* **19** (2000), 3182–3192.

[17] R.T. Cormier, K.H. Hong, R.B. Halberg et al., Secretory phospholipase Pla2g2a confers resistance to intestinal tumorigenesis, *Nat. Genet.* **17** (1997), 88–91.

[18] P.A. Croonquist, M.A. Linden, F. Zhao et al., Gene profiling of a myeloma cell line reveals similarities and unique signatures among IL-6 response, N-ras-activating mutations, and coculture with bone marrow stromal cells, *Blood* **102** (2003), 2581–2592.

[19] P. Demant, Cancer susceptibility in the mouse: genetics, biology and implications for human cancer, *Nat. Rev. Genet.* **4** (2003), 721–734.

[20] S.D. Der, A. Zhou, B.R. Williams et al., Identification of genes differentially regulated by interferon alpha, beta, or gamma using oligonucleotide arrays, *Proc. Natl. Acad. Sci. USA* **95** (1998), 15623–15628.

[21] W.F. Dietrich, E.S. Lander, J.S. Smith et al., Genetic identification of Mom-1, a major modifier locus affecting Min-induced intestinal neoplasia in the mouse, *Cell* **75** (1993), 631–639.

[22] A. Fichera, N. Little, S. Jagadeeswaran et al., Epidermal growth factor receptor signaling is required for microadenoma formation in the mouse azoxymethane model of colonic carcinogenesis, *Cancer Res.* **67** (2007), 827–835.

[23] R.J. Fijneman and R.T. Cormier, The roles of sPLA2-IIA (Pla2g2a) in cancer of the small and large intestine, *Front. Biosci.* **13** (2008), 4144–4174.

[24] R.J. Fijneman and P. Demant, A gene for susceptibility to small intestinal cancer, ssic1, maps to the distal part of mouse chromosome 4, *Cancer Res.* **55** (1995), 3179–3182.

[25] R.J. Fijneman, J.R. Peham, M.A. van de Wiel et al., Expression of Pla2g2a prevents carcinogenesis in Muc2-deficient mice, *Cancer Sci.* **99** (2008), 2113–2119.

[26] K. Ganesan, T. Ivanova, Y. Wu et al., Inhibition of gastric cancer invasion and metastasis by PLA2G2A, a novel beta-catenin/TCF target gene, *Cancer Res.* **68** (2008), 4277–4286.

[27] C.M. Gao, T. Takezaki, J.Z. Wu et al., Polymorphisms of alcohol dehydrogenase 2 and aldehyde dehydrogenase 2 and colorectal cancer risk in Chinese males, *World J. Gastroenterol.* **14** (2008), 5078–5083.

[28] R.C. Gentleman, V.J. Carey, D.M. Bates et al., Bioconductor: open software development for computational biology and bioinformatics, *Genome Biol.* **5** (2004), R80.

[29] A.W. Goldrath, C.J. Luckey, R. Park et al., The molecular program induced in T cells undergoing homeostatic proliferation, *Proc. Natl. Acad. Sci. USA* **101** (2004), 16885–16890.

[30] K.A. Gould, C. Luongo, A.R. Moser et al., Genetic evaluation of candidate genes for the Mom1 modifier of intestinal neoplasia in mice, *Genetics* **144** (1996), 1777–1785.

[31] D. Greetham, C.D. Ellis, D. Mewar et al., Functional characterization of NF-kappaB inhibitor-like protein 1 (NFkappaBIL1), a candidate susceptibility gene for rheumatoid arthritis, *Hum. Mol. Genet.* **16** (2007), 3027–3036.

[32] K. Guda, K.P. Claffey, M. Dong et al., Defective processing of the transforming growth factor-beta1 in azoxymethane-induced mouse colon tumors, *Mol. Carcinog.* **37** (2003), 51–59.

[33] K. Guda, H. Cui, S. Garg et al., Multistage gene expression profiling in a differentially susceptible mouse colon cancer model, *Cancer Lett.* **191** (2003), 17–25.

[34] T. Hanada, T. Kobayashi, T. Chinen et al., IFNgamma-dependent, spontaneous development of colorectal carcinomas in SOCS1-deficient mice, *J. Exp. Med.* **203** (2006), 1391–1397.

[35] D. Hartl, S. Krauss-Etschmann, B. Koller et al., Infiltrated neutrophils acquire novel chemokine receptor expression and chemokine responsiveness in chronic inflammatory lung diseases, *J. Immunol.* **181** (2008), 8053–8067.

[36] K. Hata, Y. Yamada, T. Kuno et al., Tumor formation is correlated with expression of beta-catenin-accumulated crypts in azoxymethane-induced colon carcinogenesis in mice, *Cancer Sci.* **95** (2004), 316–320.

[37] T. Hinoi, M. Loda and E.R. Fearon, Silencing of CDX2 expression in colon cancer via a dominant repression pathway, *J. Biol. Chem.* **278** (2003), 44608–44616.

[38] S. Holmes, A.M. Downs, A. Fosberry et al., Sema7A is a potent monocyte stimulator, *Scand. J. Immunol.* **56** (2002), 270–275.

[39] K. Ishiguro, T. Ando, O. Maeda et al., Paeonol attenuates TNBS-induced colitis by inhibiting NF-kappaB and STAT1 transactivation, *Toxicol. Appl. Pharmacol.* **217** (2006), 35–42.

[40] M. Jechlinger, S. Grunert, I.H. Tamir et al., Expression profiling of epithelial plasticity in tumor progression, *Oncogene* **22** (2003), 7155–7169.

[41] Y. Katoh and M. Katoh, Hedgehog signaling, epithelial-to-mesenchymal transition and miRNA (review), *Int. J. Mol. Med.* **22** (2008), 271–275.

[42] Y. Katoh and M. Katoh, Integrative genomic analyses on GLI2: mechanism of Hedgehog priming through basal GLI2 expression, and interaction map of stem cell signaling network with P53, *Int. J. Oncol.* **33** (2008), 881–886.

[43] E. Lapi, S. Di Agostino, S. Donzelli et al., PML, YAP, and p73 are components of a proapoptotic autoregulatory feedback loop, *Mol. Cell* **32** (2008), 803–814.

[44] S.Y. Leung, X. Chen, K.M. Chu et al., Phospholipase A2 group IIA expression in gastric adenocarcinoma is associated with prolonged survival and less frequent metastasis, *Proc. Natl. Acad. Sci. USA* **99** (2002), 16203–16208.

[45] D. Levy, N. Reuven and Y. Shaul, A regulatory circuit controlling Itch-mediated p73 degradation by Runx, *J. Biol. Chem.* **283** (2008), 27462–27468.

[46] G. Liang, F.A. Gonzales, P.A. Jones et al., Analysis of gene induction in human fibroblasts and bladder cancer cells exposed to the methylation inhibitor 5-aza-2′-deoxycytidine, *Cancer Res.* **62** (2002), 961–966.

[47] M. Lindstedt, B. Johansson-Lindbom and C.A. Borrebaeck, Global reprogramming of dendritic cells in response to a concerted action of inflammatory mediators, *Int. Immunol.* **14** (2002), 1203–1213.

[48] M. MacPhee, K.P. Chepenik, R.A. Liddell et al., The secretory phospholipase A2 gene is a candidate for the Mom1 locus, a major modifier of ApcMin-induced intestinal neoplasia, *Cell* **81** (1995), 957–966.

[49] L.W. Maines, L.R. Fitzpatrick, K.J. French et al., Suppression of ulcerative colitis in mice by orally available inhibitors of sphingosine kinase, *Dig. Dis. Sci.* **53** (2008), 997–1012.

[50] M. Markova, R.A. Koratkar, K.A. Silverman et al., Diversity in secreted PLA2-IIA activity among inbred mouse strains that are resistant or susceptible to Apc Min/+ tumorigenesis, *Oncogene* **24** (2005), 6450–6458.

[51] K. Matsuo, N. Hamajima, T. Hirai et al., Aldehyde dehydrogenase 2 (ALDH2) genotype affects rectal cancer susceptibility due to alcohol consumption, *J. Epidemiol.* **12** (2002), 70–76.

[52] A.G. McLennan, The Nudix hydrolase superfamily, *Cell Mol. Life Sci.* **63** (2006), 123–143.

[53] P. Minoo, I. Zlobec, K. Baker et al., Prognostic significance of mammalian sterile20-like kinase 1 in colorectal cancer, *Mod. Pathol.* **20** (2007), 331–338.

[54] V.K. Mootha, C.M. Lindgren, K.F. Eriksson et al., PGC-1alpha-responsive genes involved in oxidative phosphorylation are coordinately downregulated in human diabetes, *Nat. Genet.* **34** (2003), 267–273.

[55] H. Nagayoshi, A. Matsumoto, R. Nishi et al., Increased formation of gastric N(2)-ethylidene-2′-deoxyguanosine DNA adducts in aldehyde dehydrogenase-2 knockout mice treated with ethanol, *Mutat. Res.* **673** (2009), 74–77.

[56] P.R. Nambiar, M. Nakanishi, R. Gupta et al., Genetic signatures of high- and low-risk aberrant crypt foci in a mouse model of sporadic colon cancer, *Cancer Res.* **64** (2004), 6394–6401.

[57] N.F. Paoni, M.W. Feldman, L.S. Gutierrez et al., Transcriptional profiling of the transition from normal intestinal epithelia to adenomas and carcinomas in the APCMin/+ mouse, *Physiol. Genomics* **15** (2003), 228–235.

[58] A. Papanikolaou, Q.S. Wang, D.A. Delker et al., Azoxymethane-induced colon tumors and aberrant crypt foci in mice of different genetic susceptibility, *Cancer Lett.* **130** (1998), 29–34.

[59] S. Radaeva, B. Jaruga, F. Hong et al., Interferon-alpha activates multiple STAT signals and down-regulates c-Met in primary human hepatocytes, *Gastroenterology* **122** (2002), 1020–1034.

[60] R. Ramasawmy, K.C. Fae, E. Cunha-Neto et al., Variants in the promoter region of IKBL/NFKBIL1 gene may mark susceptibility to the development of chronic Chagas' cardiomyopathy among Trypanosoma cruzi-infected individuals, *Mol. Immunol.* **45** (2008), 283–288.

[61] T.R. Sana, M.J. Janatpour, M. Sathe et al., Microarray analysis of primary endothelial cells challenged with different inflammatory and immune cytokines, *Cytokine* **29** (2005), 256–269.

[62] O.J. Sansom, K.R. Reed, A.J. Hayes et al., Loss of Apc in vivo immediately perturbs Wnt signaling, differentiation, and migration, *Genes Dev.* **18** (2004), 1385–1390.

[63] G.K. Smyth, Linear models and empirical Bayes methods for assessing differential expression in microarray experiments, *Stat. Appl. Genet. Mol. Biol.* **3** (2004), Article 3.

[64] N.M. Sorensen, M. Kobaek-Larsen, A. Bonne et al., Analysis of beta-catenin, Ki-ras, and microsatellite stability in azoxymethane-induced colon tumors of BDIX/Orl Ico rats, *Comp. Med.* **53** (2003), 633–638.

[65] A. Subramanian, P. Tamayo, V.K. Mootha et al., Gene set enrichment analysis: a knowledge-based approach for interpreting genome-wide expression profiles, *Proc. Natl. Acad. Sci. USA* **102** (2005), 15545–15550.

[66] R. Suzuki, H. Kohno, S. Sugie et al., Strain differences in the susceptibility to azoxymethane and dextran sodium sulfate-induced colon carcinogenesis in mice, *Carcinogenesis* **27** (2006), 162–169.

[67] M. Takahashi, S. Nakatsugi, T. Sugimura et al., Frequent mutations of the beta-catenin gene in mouse colon tumors induced by azoxymethane, *Carcinogenesis* **21** (2000), 1117–1120.

[68] A. Takeda, C. Goolsby and N.R. Yaseen, NUP98-HOXA9 induces long-term proliferation and blocks differentiation of primary human CD34+ hematopoietic cells, *Cancer Res.* **66** (2006), 6628–6637.

[69] H. Yamaguchi, K. Bhalla and H.G. Wang, Bax plays a pivotal role in thapsigargin-induced apoptosis of human colon cancer HCT116 cells by controlling Smac/Diablo and Omi/HtrA2 release from mitochondria, *Cancer Res.* **63** (2003), 1483–1489.

[70] Z. Yang, X. Zhang, H. Gang et al., Up-regulation of gastric cancer cell invasion by Twist is accompanied by N-cadherin and fibronectin expression, *Biochem. Biophys. Res. Commun.* **358** (2007), 925–930.

[71] F. Zhan, Y. Huang, S. Colla et al., The molecular classification of multiple myeloma, *Blood* **108** (2006), 2020–2028.

[72] H. Zhao, L.E. Wang, D. Li et al., Genotypes and haplotypes of ERCC1 and ERCC2/XPD genes predict levels of benzo[a]pyrene diol epoxide-induced DNA adducts in cultured primary lymphocytes from healthy individuals: a genotype-phenotype correlation analysis, *Carcinogenesis* **29** (2008), 1560–1566.

[73] H. Zhu, J.P. Cong, G. Mamtora et al., Cellular gene expression altered by human cytomegalovirus: global monitoring with oligonucleotide arrays, *Proc. Natl. Acad. Sci. USA* **95** (1998), 14470–14475.